

UnifSrv: AP Selection for Achieving Uniformly Good Performance of CF-MIMO in Realistic Urban Networks

Yunlu Xiao, Marina Petrova, and Ljiljana Simić

Abstract—Under the ideal assumption of uniform propagation, cell-free massive MIMO (CF-mMIMO) provides uniformly high throughput over the network by effectively surrounding each user with its serving access point (AP) set. However, in realistic non-uniform urban propagation environments, it is difficult to consistently select good limited serving AP sets, resulting in significantly degraded throughput, reintroducing “edge-effect” for the worst-served users. To restore the uniformly good performance of scalable CF-mMIMO in realistic urban networks, we formulate a novel multi-objective optimization problem to jointly achieve high throughput by maximizing the sum data rate, uniform throughput by maximizing Jain’s fairness index of the throughput per user, and scalability by minimizing the serving AP set size. We then propose the *UnifSrv* AP selection algorithms to solve this optimization problem, consisting of a deep reinforcement learning (DRL)-based algorithm *UnifSrv-DRL* and a heuristic algorithm *UnifSrv-heu*. We conduct a comprehensive performance evaluation of scalable CF-mMIMO under realistic urban network distributions, propagation, and mobility patterns, showing that the prior benchmark AP selection schemes fail to provide uniformly high throughput in practice. By contrast, *UnifSrv* at least doubles the throughput compared to prior benchmarks, or achieves comparable throughput but with half of the serving AP set size. Importantly, our heuristic algorithm achieves equivalent throughput to our DRL one, but with orders of magnitude lower complexity. We thus for the first time propose an AP selection algorithm that achieves uniformly good CF-mMIMO performance in realistic urban networks with low complexity.

Index Terms—cell-free massive MIMO, serving AP selection, distributed MIMO, realistic urban propagation

I. INTRODUCTION

Cell-free massive multiple-input-multiple-output (CF-mMIMO) has been proposed [1] to achieve ubiquitous connectivity over the entire network by coordinating all access points (APs) to jointly serve all users (UEs). Different from the traditional cellular network, where a UE is only served by one base station [2], CF-mMIMO deploys dense APs over the network to form a distributed MIMO array to serve all UEs. In this case, all UEs in the network achieve significantly *higher* throughput compared to the cellular network due to the diversity gain of massive MIMO and *more uniform* throughput due to the removal of cell boundaries and the cell-edge effect for the worst-served UEs [3]. However, managing the entire network to simultaneously serve a given UE results in impractical signaling overhead and system costs. Scalable CF-mMIMO is thus proposed in [4] to reduce the overheads and still preserve the high and uniform throughput

The authors are with the Chair of Mobile Communications and Computing at RWTH Aachen University, Aachen 52072, Germany (email: {yunlu.xiao, petrova, simic}@mcc.rwth-aachen.de).

by serving a given UE with a subset of APs with the best channel conditions. Many algorithms have been proposed [5–11] to effectively select this best serving subset for each UE. However, these works assume a random uniform distribution of APs and UEs (according to a Poisson point process (PPP)) and a distance-dependent path loss model, whereby the channel conditions over the network are by default assumed to be uniformly distributed. Therefore, when all UEs are served by APs with the best channel conditions to them - corresponding to the UE being effectively surrounded by its AP serving set - their throughput performance will be *uniformly good*, as envisioned in original CF-mMIMO. Namely, under the ideal assumptions of PPP distributed nodes and a distance-based path loss model, fairness in throughput among all UEs is inherently achieved and thus not considered in the AP selection algorithm design in the existing literature [5–11].

However, we point out in [12] that the layout of realistic network deployments and the associated propagation environments in urban areas are highly non-uniform, leading to a significant degradation in the throughput performance of CF-mMIMO. Under realistic propagation, the channel conditions are generally worse than in an ideal uniform network due to building shadowing. In this case, the existing AP selection algorithms that aim at maximizing the throughput [5–7] will select a very large number of serving APs to achieve the required serving set channel quality; thus results in poor scalability, i.e., a very large serving set size and thus high system cost. On the other hand, the algorithms aiming to form a limited serving AP set that surrounds the UE [8–10] will obtain significantly lower throughput due to bad serving set quality. Finally, the algorithm in [11] that aims at both high throughput and limited serving set size by reducing the AP-UE connections with bad channels will trade off the throughput of the worst-served UEs for a small serving set size. This leads to a non-uniform throughput distribution over the network, in contrast to the design of CF-mMIMO. Therefore, it is vital to reconsider AP selection in realistic urban environments to make CF-mMIMO work in practice. Importantly, the uniformly high throughput promised by CF-mMIMO over the whole network should not be assumed by default in the highly non-uniform urban propagation environments. Instead, besides the throughput and system cost, the *fairness* in throughput performance among UEs should be explicitly studied and optimized during the AP selection for CF-mMIMO in realistic urban environments. However, to the best of our knowledge, realistic network distributions and propagation are far unaddressed in AP selection for CF-mMIMO, putting into

question whether CF-mMIMO can in fact achieve both high and uniform throughput in practical mobile networks.

To address this important gap, we present a comprehensive study of the performance of CF-mMIMO under realistic urban propagation environments and show that the existing AP selection methods in [5–11, 13] fail to achieve uniformly high throughput. To provide a solution for CF-mMIMO in realistic urban networks, we introduce Jain’s fairness index to quantify the uniformity of throughput over the network. We then formulate a novel multi-objective optimization problem to jointly maximize the throughput, maximize the fairness index, and minimize the AP-UE connections. We propose the solution to this optimization problem as *UnifSrv*, novel serving AP selection algorithms that achieve both high and uniform throughput under highly non-uniform urban propagation, consisting of a deep reinforcement learning (DRL)-based algorithm *UnifSrv-DRL* and a low-complexity heuristic algorithm *UnifSrv-heu*.

Our key contributions are:

- We conduct a comprehensive performance analysis of CF-mMIMO under realistic urban network distributions and UE mobility patterns, in propagation environments as given by a site-specific raytracing channel in Seoul and Frankfurt. Our results show that the benchmark AP selection schemes for CF-mMIMO obtain significantly worse throughput in realistic urban environments than in ideal PPP networks, and thus fail to provide uniformly good performance of CF-mMIMO in practice.
- We formulate and solve a novel multi-objective optimization problem to design *UnifSrv*, AP selection algorithms that achieve *uniformly good* throughput for CF-mMIMO under realistic urban propagation. We maximize both the total throughput and Jain’s fairness index of the throughput per UE, and minimize the number of AP-UE connections. We also constrain both the serving AP set size per UE and the number of served UEs per AP to achieve scalability.
- We propose the *UnifSrv-DRL* algorithm by designing a deep Q-learning framework to solve the transformed multi-objective optimization problem. We then propose a dynamic threshold-based heuristic algorithm *UnifSrv-heu* by introducing a fairness index-based threshold to control the serving AP set expansion. Both of our *UnifSrv* algorithms significantly outperform all considered existing AP selection algorithms and successfully achieve uniformly high throughput for scalable CF-mMIMO under realistic propagation.
- Importantly, our heuristic algorithm *UnifSrv-heu* achieves equivalently good throughput performance as *UnifSrv-DRL*, but with orders of magnitude lower algorithm complexity. We thus for the first time propose an AP selection algorithm that achieves both high and uniform throughput of scalable CF-mMIMO in realistic urban environments with low complexity, making CF-mMIMO viable for practical mobile networks.

The rest of this paper is organized as follows: Sec. II reviews the related work on AP selection in CF-mMIMO, Sec. III details the system model, Sec. IV proposes our *UnifSrv*

algorithms, Sec. V evaluates the performance of our algorithms and other benchmarks, and Sec. VI concludes the paper.

II. RELATED WORK

The performance of CF-mMIMO under realistic urban environments is largely unaddressed in the existing literature, with only a few exceptions [12, 14–18]. The works in [14, 15] take into account the site-specific AP locations in the cities of Seoul and Frankfurt to show the realistic AP location itself already has an impact on the throughput of CF-mMIMO. However, they still model the path loss by a log-distance model and do not consider the impact of realistic propagation. The work in [16] studies a site-specific channel corresponding to CF-mMIMO systems via measurements and [17] studies realistic urban propagation of a mm-wave system via raytracing, showing that the CF-mMIMO architecture indeed achieves channel hardening in realistic multipath propagation. However, neither of them considers any network-wide throughput performance analysis or AP selection. Our work in [12] studies the significant throughput performance difference of scalable CF-mMIMO between the widely-assumed log-distance path loss model and the realistic raytracing propagation model, assuming the simple AP selection method from [8], but without providing solutions to close the performance gap. The work in [18] considers a CF-mMIMO network in an area of Tokyo with a raytracing channel model and mobile UEs and proposes a DRL-based AP selection. However, this algorithm solely aims at reducing the signalling and computational complexity, while the achieved throughput is much lower than the fixed-size AP selection. By contrast, in this paper we for the first time conduct a comprehensive performance analysis of scalable CF-mMIMO using various AP selection schemes in [5, 8, 11, 13] in realistic urban networks, whereby we jointly consider realistic distributions, propagation, and mobility patterns. We then propose two novel AP selection algorithms that achieve uniformly high throughput for scalable CF-mMIMO in realistic urban networks.

Many works studied serving AP set selection for CF-mMIMO in a static network with a PPP distribution and log-distance path loss model. The works in [5–7] propose *pure UE-centric (PUC)* algorithms that focus on maximizing the throughput. In [5] a large-scale-fading-based algorithm is proposed to maximize the throughput per UE by selecting the APs with the highest received signal strength to serve a given UE until the total channel gain of the serving set achieves 95% of the channel gain where all APs serve the UE. A deep deterministic policy gradient algorithm is proposed in [6] to both maximize the total throughput over the network and satisfy the minimum required throughput, and therefore especially improve the throughput of the poorly-performing UEs compared to the fixed-size AP selection. Similarly, AP selection based on federated multi-agent reinforcement learning is proposed in [7] to maximize both the sum throughput and the throughput of worst-served UEs. However, these algorithms do not consider the serving AP set size constraint of scalable CF-mMIMO. We show in Sec. V-A that the *PUC* benchmark thus obtains very large serving sets under the realistic urban environment, in order to achieve a high serving set quality with generally poor channels.

TABLE I
RELATED WORK ON AP SELECTION FOR CF-MMIMO.

Reference	Maximize throughput	Constrain AP serving set size	Model fairness	Reduce pilot contamination	Realistic propagation
[5–7], <i>PUC</i>	✓	✗	✗	✗	✗
[8–10], <i>CUC</i>	✗	✓	✗	✗	✗
[11], <i>PUC-const</i>	✓	✗	✗	✓	✗
[13] (cellular), <i>PF-DRL</i>	✗	✓	✓	✓	✗
This paper, <i>UnifSrv</i>	✓	✓	✓	✓	✓

The works in [8–10] consider limiting the serving AP set size. The *clustered UE-centric (CUC)* algorithms are proposed in [8, 9] to constrain the serving AP set size per UE by assigning the APs to multiple disjoint clusters and then serving the UEs with a limited number of clusters. In particular, a heuristic algorithm is proposed in [8], where the UEs are served by the few clusters to which the APs with the best channels belong. A Gaussian Mixture Model algorithm is proposed in [9] to optimize the serving cluster selection to achieve both high average and 90%-likely throughput. A DRL-based algorithm is proposed in [10] to minimize the AP-UE connections and achieve high throughput with reduced fronthaul requirements. However, these designs assume the channel conditions of all APs in a similar location, e.g., in the same cluster, to be similar; this does not hold under realistic propagation [12]. We show in Sec. V-A that these algorithms result in a low throughput under realistic urban propagation.

A *constrained pure UE-centric (PUC-const)* algorithm is proposed in [11] to constrain the number of served UEs to the available number of pilots per AP, and therefore both achieve a serving set with good channel conditions for UEs and reduce pilot contamination for APs. A DRL-based algorithm *PF-DRL* is proposed in [13] to optimize the proportional fairness of throughput per UE¹ and achieve uniform throughput over the network. However, we show in Sec. V-A that *PUC-const* trades off the throughput of the worst-served UEs to satisfy the constraint, leading to a non-uniform throughput performance. On the other hand, *PF-DRL* trades off the throughput of the well-served UEs to achieve proportional fairness, resulting in low sum throughput over the network.

Overall, these prior algorithms [5–11, 13] consider the objective of maximizing throughput, limiting serving set size, reducing pilot contamination, or achieving uniform throughput *separately*. By contrast, our work *jointly* considers all these objectives and constraints, optimizing the throughput of the poorly-performing UEs by optimizing the throughput performance fairness over the whole network, thus achieving high *and* uniform throughput across the network. Finally we note that the prior algorithms in [5–7, 10, 11] are based on the impractical UE-centric CF-mMIMO architecture with only one central processing unit (CPU) managing the entire network, while the works in [8, 9] assume multiple CPUs in the network but only form the serving set with complete CPU clusters. By contrast, we consider the practical open radio access network (O-RAN) architecture proposed in [19] with

¹We note that the algorithm in [13] is designed for UE and base station association in a cellular network, but the methodology can be expanded to CF-mMIMO AP selection. We thus also consider it as a benchmark AP selection scheme giving it explicitly maximizes the proportional fairness of data rate. The *PF-DRL* algorithm for CF-mMIMO will be detailed in Sec. IV-C.

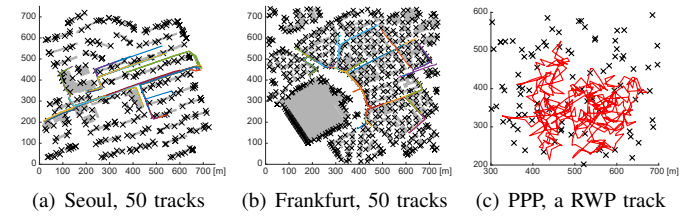


Fig. 1. Network topologies and UE mobility patterns, with buildings marked with gray polygons, AP locations marked with black crosses, and UE tracks marked with colored lines (not all tracks individually visible due to overlap).

multiple CPUs in the network, and decouple the serving AP set and the CPU cluster by allowing the UE to be served by a subset of APs in a CPU cluster as in [19]. We summarize the related work on AP selection of CF-mMIMO in Table I.

III. SYSTEM MODEL

A. Network Topology & Mobility Model

We consider a network with M static APs (AP set denoted as \mathcal{M}) and K mobile UEs (\mathcal{K}) distributed in an area S , i.e., with AP density of $\lambda = M/S$ and UE density of $\lambda_U = K/S$. We consider two real city areas in Seoul and Frankfurt with qualitatively dissimilar layouts, representing different urban build-up densities, as our study areas. The building layouts are obtained via a public open data base as shapefiles [20]. We consider $M = 324$ APs ($\lambda = 576$ AP/km²) corresponding to a medium-density urban network in Seoul and $M = 625$ APs ($\lambda = 1111$ AP/km²) corresponding to a high-density urban network in Frankfurt [14]. We generate the AP locations via the AP placement algorithm in [12], whereby the APs are distributed as uniformly as possible to best achieve the ideal “cell-free” deployment [1], but we ensure the AP locations to be practical by only placing the APs at edges or corners of the building.

In addition to realistic AP distributions, we also consider practical UE mobility patterns to obtain realistic propagation for these UE locations and also consider channel aging to quantify the throughput under mobility². We generate these mobility patterns for each UE via VisWalk [23] for the two city areas based on their building layouts, where individual UE tracks are often very similar. We show in Fig. 1(a) the network topology and mobility patterns of all $K = 50$ UEs in Seoul and those in Frankfurt in Fig. 1(b). As a reference, we also consider the scenario with a PPP distribution of the M APs and the random way point (RWP) mobility model

²We note that mobility management and the handover algorithm are also important in mobile CF-mMIMO [7, 15, 21, 22]. For mobile CF-mMIMO, AP selection algorithms select the best candidate serving APs at every time step, while the handover algorithm can be applied subsequently to decide whether the serving set will be changed to the candidate set, as in [7, 15, 21, 22]. Handover algorithm design can thus be considered independent of AP selection and is out of the scope of this paper.

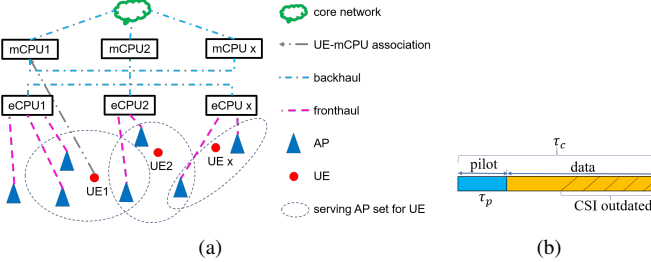


Fig. 2. Illustrations of (a) scalable CF-mMIMO architecture, (b) downlink communication block.

[24] for the K UEs in the network. We assume the UEs move with a fixed speed during each mobility period, with a random direction and Rayleigh distributed transition lengths. We show in Fig. 1(c) an example RWP UE track in a subarea of S .

B. CF-mMIMO Network Architecture

We consider the downlink of a scalable CF-mMIMO architecture based on O-RAN as in [19], which allows assigning each UE an arbitrary limited serving AP set. Fig. 2 illustrates the network architecture and downlink communication block. The APs are managed in clusters and connected to the edge CPU (eCPU) of the cluster via fronthaul. The eCPUs connect to each other and to the manager CPUs (mCPUs) and eventually to the core network via backhaul. To avoid unlimited signaling and precoding complexity, each UE is served by a subset of APs, which can be managed by multiple eCPUs. However, a UE is only associated with one mCPU for signal processing [19]. We adopt the dynamic cooperation matrix in [25] to describe the connections between all APs and UEs over the network. We define the $M \times K$ cooperation matrix as D . If AP m serves UE k , $D_{mk} = 1$, otherwise $D_{mk} = 0$. We denote the serving set size per UE k as $G_k = \sum_{m=1}^M D_{mk}$ and the number of served UEs per AP m as $W_m = \sum_{k=1}^K D_{mk}$.

We assume D is known to all CPUs so that each mCPU and eCPU is aware of its associated UEs and APs via D . For downlink transmission, the mCPU distributes the UE data to the associated eCPUs of this UE. The eCPUs then perform multi-UE precoding for the served UEs. For example, in Fig. 2(a), UE 1 is served by the APs in eCPU clusters 1 & 2 and is managed by mCPU 1. The mCPU 1 then distributes the downlink data for UE 1 to eCPU 1 & 2, letting eCPU 1 & 2 calculate precoding vectors and distribute the data to the APs they manage. The APs do not perform any processing, but only act as remote radio heads and wirelessly relay the signal from the eCPU to the UE.

C. Channel Model

We consider a downlink communication block as in Fig. 2(b) with a total length of $\tau_c = 200$ and assume the channel measurement, AP selection, and signal processing only happen every τ_c slots. Since the channels are only measured at the beginning of the communication block, channel information is outdated within the block and the channel realizations at different time instants in a block are different due to UE mobility. To model this channel aging effect, we assume the channel realizations at different time instants in a block are correlated as modelled in [26]. We further assume

TABLE II
RAYTRACING SIMULATION PARAMETERS

Parameter	Value
carrier frequency	2 GHz
bandwidth, B	20 MHz
noise figure	9 dB
antenna	Half-wave dipole
building material	ITU Concrete 2.4 GHz
propagation model	X3D raytracing
number of reflections/diffractions	6/1
outage threshold	-250 dBm

the correlation coefficient between the channel realizations at time 0 and time instant t is modelled as the zeroth-order Bessel function of the first kind [26]

$$p[t] = J_0 \left[2\pi \frac{v f_c}{c} T_s (t - \tau_p - 1) \right], \quad (1)$$

where v is the speed of the UE, c is the speed of light, T_s is the sampling time (i.e., the duration for one slot), and τ_p is the length of the pilot sequence. The channel between AP m and UE k at time t is thus [26]

$$h_{mk}[t] = p[t]h_{mk}[0] + \sqrt{1 - p^2[t]}g_{mk}[t], \quad (2)$$

where $h_{mk}[0]$ is the channel at time 0, i.e., the initial state, and $g_{mk}[t]$ is the component that is independent of channel aging. Assuming Rayleigh fading for the small-scale fading model, we have $h_{mk}[0] \sim N_C(0, R_{mk})$ and $g_{mk}[t] \sim N_C(0, R_{mk})$, where $R_{mk} = 1/L_{mk}$ represents the large-scale fading of the link between AP m and UE k [25], where L_{mk} is the path loss.

We obtain the average path loss L_{mk} in two ways. First, for our realistic urban areas of Seoul and Frankfurt, we obtain the large-scale path loss via raytracing as a deterministic channel model realistically representing the site-specific wireless propagation environment. We obtain the channel data using the Wireless Insite software from RemCom [27], based on the city layouts (cf. Fig. 1) and the simulation settings in Table II. Second, as a reference, we consider the widely adopted Hata-COST231 three-slope log-distance propagation model [1] for the PPP networks as a more simplistic statistical channel model, as typically assumed in the prior literature. This model gives the path loss with shadowing between AP m and UE k as $L_{mk} = \bar{L}_{mk} 10^{\sigma z_{mk}/10}$, with σ as the shadowing standard deviation, $z_{mk} \sim N(0, 1)$, and the average path loss in dB given by

$$\bar{L}_{mk} = \begin{cases} L_0 + 35 \log_{10}(d_{mk}), & d_{mk} > d_c \\ L_0 + 15 \log_{10}(d_c) + 20 \log_{10}(d_0), & d_{mk} \leq d_0, \\ L_0 + 15 \log_{10}(d_c) + 20 \log_{10}(d_{mk}), & \text{otherwise} \end{cases} \quad (3)$$

where d_{mk} is the distance between AP m and UE k , and

$$L_0 = 46.3 + 33.9 \log_{10}(f_c) - 13.82 \log_{10}(a_{AP}) - (1.1 \log_{10}(f_c) - 0.7) a_{UE} + (1.56 \log_{10}(f_c) - 0.8), \quad (4)$$

where f_c is the carrier frequency, a_{AP} is the AP antenna height, a_{UE} is the UE antenna height, $d_c = 50$ m, and $d_0 = 10$ m.

D. Signal Processing & Throughput Model

For signal processing, we assume a randomly assigned pilot sequence occupying $\tau_p = 10$ slots in each communication

block, minimum mean-square error (MMSE) channel estimation, equal power allocation, and partial MMSE precoding [25]. The received signal at UE k for the downlink at time t is modelled as

$$x_k[t] = \sum_{m=1}^M h_{mk}[t] \left(\sum_{i=1}^K \sqrt{p_{mi}} D_{mi} w_{mi} q_{mi} \right) + n_0, \quad (5)$$

where p_{mi} is the downlink transmit power, $q_{mi} \sim N_C(0, 1)$ is the downlink transmit signal, and w_{mi} is the precoding vector of AP m for UE i given by (18) in [26].

With the MMSE channel estimation, the channel estimate is given by $\hat{h}_{mk}[t] \sim N_C(0, Z_{mk}[t])$ [26], where

$$Z_{mk}[t] = \frac{\rho^2 [\tau_p + 1 - t] \beta_{mk}^2 n_0}{p_{mk} \sum_{k \in \mathcal{P}_k} \beta_{mk} n_0 + p_{mk}}, \quad (6)$$

with \mathcal{P}_k as the UE set that uses the same pilot as UE k ; (6) thus models the channel aging effect in channel estimation and consequently the throughput performance as follows.

With centralized partial MMSE precoding, the eCPUs (cf. Sec. III-B) calculate the precoding vector w_{mk} using the channel estimates $\hat{h}_{mk}[t]$ given by (6). The serving eCPUs then precode the signal with w_{mk} to obtain $x_k[t]$. Given the received signal in (5) and this precoding process, the signal-to-interference-and-noise ratio (SINR) for UE k is given by [26]

$$\gamma_k = \frac{\zeta}{I + n_0}, \quad (7)$$

where

$$\zeta = \rho^2 [t - \tau_p - 1] p_{mk} \left| \mathbb{E} \left\{ \sum_{m=1}^M h_{mk}^H[t] D_{mk} w_{mk} \right\} \right|^2. \quad (8)$$

$$I = \sum_{i=1}^K p_{mi} \mathbb{E} \left\{ \left| \sum_{m=1}^M h_{mk}^H[t] D_{mi} w_{mi} \right|^2 \right\} - S^d$$

The throughput of UE k is then given by [19]

$$R_k = B \frac{\tau_c - \tau_p}{\tau_c} \log(\gamma_k + 1), \quad (9)$$

where B is the system bandwidth.

IV. AP SELECTION FOR CF-MMIMO UNDER REALISTIC URBAN PROPAGATION

A. Problem Formulation

In the ideal PPP networks with uniform channel conditions, the existing AP selection algorithms in [5–11, 13] inherently achieve uniformly good throughput with small serving set sizes, even though they consider the objectives of high throughput, uniform performance, or limited serving set size separately. However, under realistic urban propagation, the channel conditions are highly non-uniform and generally worse than in an ideal PPP network [12]. We will show in Sec. V-A that these prior benchmark AP selection algorithms consequently perform poorly in realistic urban environments due to their incomplete objective consideration. Specifically, the *PUC* algorithms [5–7] that only maximize the throughput result in very large serving AP sets to improve the serving set quality via AP quantity. The *CUC* algorithms [8–10] that only limit the serving set size obtain low throughput due to bad serving set quality. The *PUC-const* algorithm [11] that aims at both high throughput and limited serving set size

leads to non-uniform throughput, because it trades off the throughput of the worst-served UEs for a small serving set size. The *PF-DRL* algorithm [13] that solely maximizes the fairness leads to uniform but low throughput over the network, because it trades off the throughput of the well-served UEs to achieve proportional fairness. Therefore, it is necessary to instead jointly optimize sum throughput, per UE throughput fairness, and limiting the number of AP - UE connections for AP selection under realistic propagation to achieve uniformly good performance of scalable CF-mMIMO.

To address this gap, we formulate a novel multi-objective optimization problem for AP selection in realistic urban networks as follows. We set the high throughput objective as maximizing the total data rate, and the uniform throughput objective as maximizing Jain's fairness index [28] of the data rate per UE. The fairness index Φ is used to evaluate how fair the throughput performance of a UE is compared to other UEs in the network, with index values in the range $[1/K, 1]$. When $\Phi \rightarrow 1$, the UEs achieve similar throughput over the network and the system is considered to be fair. We also minimize the number of AP-UE connections to reduce the signaling and processing cost [25]. To avoid pilot contamination, we constrain the number of UEs served by each AP W_m to no more than the pilot length τ_p [11]. We also constrain the number of APs serving a UE G_k to $G_{max} < M$ to achieve scalability and limited system cost [25]. The decision variable D_{mk} is a binary variable that states whether AP m is connected to UE k or not. The formulation of the optimization problem is as follows:

$$\max_{D_{mk}} \sum_{k=1}^K R_k, \quad (10a)$$

$$\max_{D_{mk}} \Phi = \frac{\left(\sum_{k=1}^K R_k \right)^2}{K \sum_{k=1}^K R_k^2}, \quad (10b)$$

$$\min_{D_{mk}} \sum_{k=1}^K \sum_{m=1}^M D_{mk}, \quad (10c)$$

$$\text{s.t. } W_m = \sum_{k=1}^K D_{mk} \leq \tau_p, \quad \forall m \in \mathcal{M}, \quad (10d)$$

$$G_k = \sum_{m=1}^M D_{mk} \leq G_{max}, \quad \forall k \in \mathcal{K}, \quad (10e)$$

$$D_{mk} \in \{0, 1\}, \quad \forall m \in \mathcal{M}, \forall k \in \mathcal{K}. \quad (10f)$$

B. Novel UnifSrv AP Selection Algorithms

The optimization problem in (10) is a non-linear integer programming problem, which is known to be NP-hard. To solve the problem, we first transform (10) by simplifying the data rate R_k . According to (9), the data rate monotonically increases with the SINR γ_k , and therefore the optimization objectives (10a) and (10b) can be transformed to optimize the sum and fairness index of SINR per UE given in (7), i.e., replace R_k with γ_k in (10). We further use the average signal-to-noise ratio (SNR) of the channel between AP m and UE k over a communication block, given by $\beta_{mk} = p_{mk}/(L_{mk} n_0)$, to represent the channel quality during serving AP selection, since the throughput performance is correlated with the SNR [26]. We thus simplify the desired

signal ζ over noise n_0 as the sum of the average SNR of all serving AP-UE links to UE k , i.e., $\zeta/n_0 \approx \sum_{m=1}^M D_{mk}\beta_{mk}$. Similarly, the interference I over noise is simplified as the average interference-to-noise ratio of all non-serving APs to UE k , i.e., $I/n_0 \approx \sum_{m=1}^M \beta_{mk} - \sum_{m=1}^M D_{mk}\beta_{mk}$. The SINR γ_k is thus simplified as

$$\gamma_k \approx S_k = \frac{\sum_{m=1}^M D_{mk}\beta_{mk}}{\sum_{m=1}^M \beta_{mk} - \sum_{m=1}^M D_{mk}\beta_{mk} + 1}, \quad (11)$$

The objective (10a) and (10b) can finally be transformed by replacing R_k with S_k . We note that (11) is only used to relax and solve the optimization problem (10). We still use the full instantaneous SINR model in (7) in our performance evaluation in Sec. V. In the following, we propose a DRL approach *UnifSrv-DRL* and a threshold-based heuristic algorithm *UnifSrv-heu* to solve the transformed optimization problem.

1) *UnifSrv-DRL*: We propose a DRL algorithm to solve (10) as follows. We model the AP selection of CF-mMIMO as a Markov decision process (MDP), with the state s as the channel condition from all possible AP-UE connections and the action a as all the possible values of the $M \times K$ connection matrix D . We deploy one agent at the core network to learn the AP selection policy by interacting with the environment by trial and error and receiving a reward based on its actions via the optimal action-value function $Q(s, a)$. The dimension of both the state and action space grows to 2^{MK} . To avoid visiting every possible state in such a large state space, we let the agent make the connection decision of each UE one by one, so that the agent needs only to observe the channel state and serving set of a given UE k . We then use a neural network to approximate the action-value function $Q_\theta(s, a)$, i.e., we apply the DQN algorithm to perform the DRL.

State space: The state of UE k is given by $s_k = \{D_{1k}\beta_{1k}, \dots, D_{Mk}\beta_{Mk}, W_1, \dots, W_{G_{max}}\}$, which observes the channel quality of the current serving AP set in terms of β_{mk} and the serving capacity of these APs in terms of W_k .

Action space: The action space is the set of all APs that provide a sufficient SNR to UE k , given by $a_k = \{m \in 1, \dots, M | \beta_{mk} \geq \beta_0\}$, where β_0 is the SNR threshold for valid connections. The APs with an SNR below a typical decoding threshold should not be considered as a serving AP to this UE at all. We thus remove these APs from the action space to speed up the training.

DQN algorithm & reward function: At each step within an episode, the agent performs an action to connect a UE k to a random AP within the action space. For each step, we offer an immediate reward $r_1 = \omega_1 \beta_{m^*k} / \beta_{max}$, where ω_1 is a constant representing the weight, m^* is the index of the AP chosen in this action, and β_{max} is the highest SNR this UE can obtain from any AP. This reward encourages the agent to connect UE k with the APs with as good channel quality as possible. We also apply a penalty if the AP chosen cannot serve more UEs, i.e., $r_1 = -1$ if $W_{m^*} \geq \tau_p$. This teaches the agent to satisfy the constraint in (10d). After U_m steps or when the number of candidate serving APs for this UE reaches G_{max} , which we consider as one round, the agent moves on to the next UE. In this case, each UE is served by at most G_{max} APs, which satisfies the constraint in (10e). For each

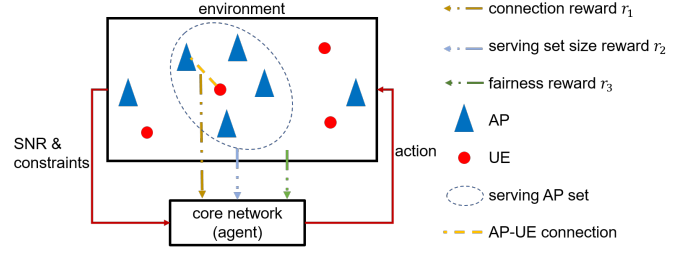


Fig. 3. The DRL-based AP selection algorithm framework of *UnifSrv-DRL*. round, we design an intermediate reward function to evaluate the serving set size, given by

$$r_2 = \omega_2 (1 - \sum_{m=1}^M D_{mk}/M), \quad (12)$$

where ω_2 is a constant. This reward encourages the agent to obtain small serving set sizes, matching the objective in (10c). At the end of one episode, the agent finishes selecting serving APs for all UEs. We provide a final reward as the weighted sum rate in (10a) scaled by the fairness index in (10b),

$$r_3 = \omega_3 \Phi' \sum_{k=1}^K S_k = \omega_3 \frac{\left(\sum_{k=1}^K S_k\right)^3}{K \sum_{k=1}^K S_k^2}, \quad (13)$$

where ω_3 is a constant representing the weight and Φ' is the Jain's fairness index of S_k . Fig. 3 illustrates the DRL-based AP selection algorithm framework.

2) *UnifSrv-heu*: We also propose the algorithm *UnifSrv-heu* in Alg. 1 as a heuristic solution to (10). In Steps 1 to 6, each UE connects to the AP with the best SNR to form the initial serving set. Then in Steps 7 to 10, a threshold α is calculated based on Jain's fairness index Φ of S_k . UEs with a simplified SINR S_k lower than α are considered to be not fairly served and require more serving APs to be allocated. Therefore, in Steps 11 to 17, these UEs are assigned the next AP with the best SNR to their serving set, as long as both the AP and UE do not exceed the constraints given by (10d) and (10e). We also stop adding APs to the serving set if the total SNR reaches $\delta\%$ of the SNR when all APs serve the UE, in order to satisfy the objective (10c). By contrast, UEs with $S_k \geq \alpha$ are considered to have already good serving sets, and therefore do not need to be assigned the additional serving AP m . When the selection of AP m is done for all UEs, α will be evaluated again for the selection of the next AP $m+1$. The algorithm satisfies the objective (10a) by always selecting the APs with the best SNR to serve, and (10b) by applying the fairness-based threshold α . Importantly, our algorithm thus prioritizes the AP selection for the worst-served UEs to improve their throughput, and thus the uniformity of the throughput performance over the CF-mMIMO network.

C. Reference AP Selection Algorithms

We here briefly present four reference AP selection algorithms as the representative benchmarks for existing works detailed in Sec. II, as follows.

PUC: The *pure UE-centric (PUC)* algorithm from [5] described in Alg. 2 is representative of the algorithms from [5–7] that only focus on maximizing the per-UE throughput. The UEs are served by the APs with the best SNR until the

Algorithm 1 UnifSrv-heu

Input: The SNR β_{mk} between AP m and UE k for $m = 1, \dots, M$ and $k = 1, \dots, K$. The zero matrix $D[t] = \mathbf{0}$. The pilot sequence length τ_p . The maximum serving set size G_{max} . The SNR percentage threshold δ .

```

1: for  $k = 1, \dots, K$  do
2:   Sort the APs in descending order based on  $\beta_{mk}[t]$ ,  $m = 1, \dots, M$ .
3:   Define the AP index in the descending order as  $\{O(1), O(2), \dots, O(M)\}$ .
4:   Set  $D_{O(1)k} = 1$ .
5:   Calculate  $S_k$  with (11).
6: end for
7: for  $m = 2, \dots, M$  do
8:   Calculate the Jain's fairness index  $\Phi$  with (10b), replace  $R_k$  with  $S_k$ .
9:   Sort  $S_k$  for all UEs in the ascending order.
10:  Set the threshold  $\alpha = S_{\lceil((1-\Phi)K)^{th}\rceil}$ .
11:  for  $k = 1, \dots, K$  do
12:    if  $S_k < \alpha$  &  $W_m \leq \tau_p$  &  $G_k \leq G_{max}$  &  $\sum_{m=1}^M D_{mk} \beta_{mk} < \delta \sum_{m=1}^M \beta_{mk}$  then
13:      Set  $D_{O(m)k} = 1$ .
14:    end if
15:    Calculate  $S_k$  with (11).
16:  end for
17: end for

```

Output: The dynamic cooperation matrix D .

total SNR reaches $\delta\%$ of the original CF-mMIMO case (i.e., when all APs serve each UE).

PUC-const: The *constrained pure UE-centric* (*PUC-const*) algorithm from [11] in Alg. 3 adds the AP capacity constraint based on the *PUC* algorithm. The candidate serving AP is still chosen according to SNR quality, and therefore this algorithm also only considers maximizing the throughput as an objective. If an AP reaches capacity, i.e., is already assigned to τ_p UEs, the algorithm compares the SNR between the new candidate UE and the worst SNR among the assigned UEs and replaces the connection if the candidate UE has a better channel.

CUC: The *clustered UE-centric* (*CUC*) algorithm from [8] described in Alg. 4 is chosen as representative of the algorithms from [8–10] that aim at limiting the serving AP set size. The area is divided into N_c disjoint square clusters and on average $Q = M/N_c$ APs are assigned to each cluster according to their locations. The network first finds E APs with the best SNR to a UE k , then the clusters these E APs belong to form the serving set of UE k . Fig. 4 illustrates example serving AP sets formed with the reference algorithms.

PF-DRL: The *proportionally-fair DRL-based* (*PF-DRL*) algorithm from [13] aims at providing proportional fairness in data rates to all UEs over the network. It applies a DRL-based solution for a single-objective optimization problem, which share the same constraints as (10d)–(10f) and the objective given by $\max_{D_{mk}} \sum_{k=1}^K \log(R_k)$. The *PF-DRL* algorithm uses the same state space, action space, and DQN algorithm designs as our *UnifSrv-DRL* given in Sec. IV-B1. However, it only has a single final reward function according to the single objective at the end of one episode. Namely, for *PF-DRL*, the intermediate rewards $r_1 = r_2 = 0$ and the final reward

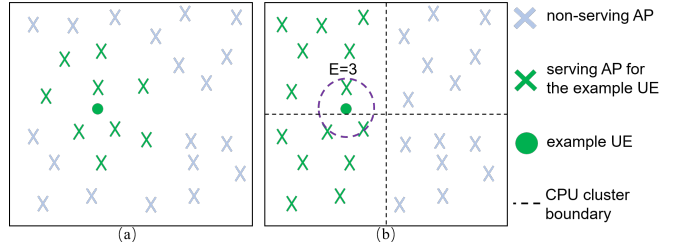


Fig. 4. An example serving AP set for a UE with (a) Alg. 2 & 3 and (b) Alg. 4, with $E = 3$, $N_c = 4$, and $Q = 7$.

TABLE III
ALGORITHM COMPLEXITY.

Algorithm	Complexity
<i>UnifSrv-DRL</i> & <i>PF-DRL</i> [13]	$\mathcal{O}(NTLn^2)$
<i>UnifSrv-heu</i> (Alg. 1)	$\mathcal{O}(K(M\log M + M\log K + M))$
<i>PUC</i> (Alg. 2 [5])	$\mathcal{O}(K(M\log M + M^2))$
<i>PUC-const</i> (Alg. 3 [11])	$\mathcal{O}(K(M\log M + M\tau_p \log \tau_p))$
<i>CUC</i> (Alg. 4 [8])	$\mathcal{O}(K(M\log M + E))$

$$r_3 = \sum_{k=1}^K \log(R_k).$$

Finally in our performance evaluation in Sec. V, we consider two boundary reference cases: the original CF-mMIMO, where all APs in the network serve all UEs (i.e., $G_k = M, \forall k$), and the small cell case, where only one AP with the best SNR serves a UE.

D. Algorithm Complexity

We give the complexity of all considered algorithms as follows. For the DQN algorithm underlying *PF-DRL* and *UnifSrv-DRL*, its complexity is dominated by the number of total training steps and the dimension of hidden layers, given by $\mathcal{O}(NTLn^2)$, where N is the number of episodes to converge, T is the number of steps in each episode, L is the number of hidden layers, and n is the dimension of the hidden layer. To train a well-performing agent for AP selection in a CF-mMIMO network with a large number of APs and UEs, n should be at least on the order of 10^2 and L on 10^3 [18], illustrating the high complexity of DRL in CF-mMIMO. The complexity of the other algorithms depends on the number of for-loops and the sorting of SNR, which depends on the network scale M and K . We give the complexity of all considered algorithms in Table III.

V. RESULTS

We conduct a comprehensive performance analysis of CF-mMIMO under realistic propagation in Sec. V-A. We then in Sec. V-B evaluate the throughput performance of our *UnifSrv* AP selection algorithms proposed in Sec. IV-B. We finally in Sec. V-C compare the overall performance and complexity of *UnifSrv* against the reference schemes in Sec. IV-C. We assume a network in an $S = 750 \text{ m} \times 750 \text{ m}$ area, with AP and UE distributions given in Sec. III-A. We assume a pedestrian UE speed of 0.8 m/s for the high density case and a cycling speed of 3.6 m/s for the low density case to represent typical urban UE mobility. We also consider the corresponding PPP distributed network with RWP mobility, with the same AP/UE density and average UE speed as the urban network as references. We simulate K UE tracks all with a mobility period of 400 s and determine the AP-UE connections every $\tau_c = 20 \text{ ms}$.

For the considered AP selection algorithms, we set $\delta = 95\%$ for the *PUC* and our *UnifSrv-heu* algorithms. For the *CUC* algorithm, we set the same average serving AP set size as the average G_k of *UnifSrv-heu*, which is obtained via simulation, for a fair comparison. Specifically, we set $\{E, Q\} = \{7, 20\}$ to achieve an average serving AP set size $G = 40$ in the network of Seoul and $\{E, Q\} = \{3, 17\}$ to achieve $G = 25$ in Frankfurt. For our *UnifSrv* algorithms and *PF-DRL*, we set the following parameters: $G_{max} = 100$ for Seoul and $G_{max} = 70$ for Frankfurt, outage SNR $\beta_0 = -20$ dB, learning rate of 10^{-5} , discount factor of 0.99, batch size of 128, buffer size of 10^6 , the total number of training episodes is 500, and the number of steps in each episode $T = KU_m$ with the number of action rounds per UE $U_m = 100$. The neural network consists of $L = 2$ hidden layers with $n = 512$ neurons each. Furthermore, we set the weights³ of the reward function of the DQN algorithm for *UnifSrv-DRL* as $\omega_1 = 1$, $\omega_2 = 10$, and $\omega_3 = 2000$.

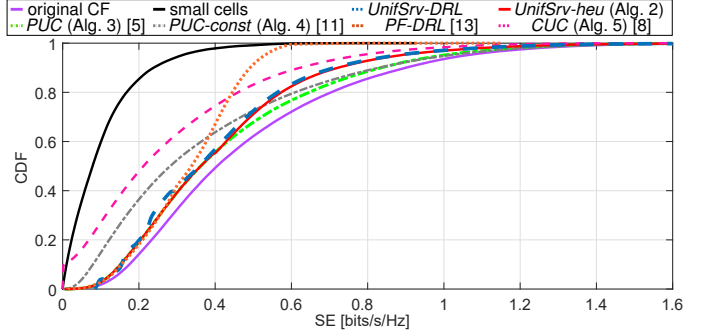
A. Throughput Performance Evaluation of CF-mMIMO Under Realistic Urban Propagation

Fig. 5 shows the distribution of the normalized throughput, i.e., spectral efficiency (SE) given by R_k/B , over all UEs and their entire mobility periods for all considered AP selection algorithms in the area of Seoul (Fig. 5(a)) and its corresponding PPP network (Fig. 5(b)). Let us first establish the performance of the two boundary cases in both urban and PPP networks: Fig. 5 confirms that the original CF-mMIMO architecture significantly improves the throughput compared to small cells. For both the Seoul and PPP networks, the sum throughput of original CF-mMIMO is four times the sum throughput of small cells. In particular, original CF-mMIMO significantly improves the throughput of the 95th percentile (i.e., worst-served) UEs. Correspondingly, original CF-mMIMO achieves a fairness index of throughput per UE of $\Phi = 0.8$ and $\Phi = 0.86$ in the Seoul and PPP networks, respectively, compared to $\Phi = 0.4$ and $\Phi = 0.5$ of small cells. The original CF-mMIMO thus achieves both *higher and more uniform* throughput than small cells, in both the Seoul and PPP networks. Moreover, comparing Fig. 5(a) to Fig. 5(b) shows that both architectures achieve significantly lower throughput in the urban case than in the PPP network. This throughput gap⁴ is caused by the channel quality difference illustrated in Fig. 6. Different from the uniform spatial distribution of the SNR in the PPP network with the log-distance path loss model shown in Fig. 6(a), Figs. 6(b) and 6(c) show that a large number of AP-UE links obtain very low SNR due to building shadowing in the urban areas. Namely, in realistic urban propagation, the channel quality is in general worse and more non-uniformly distributed than in PPP networks, as shown in Fig. 6(d). Consequently, the SE of both CF-mMIMO and small cells degrades in the case of realistic urban propagation.

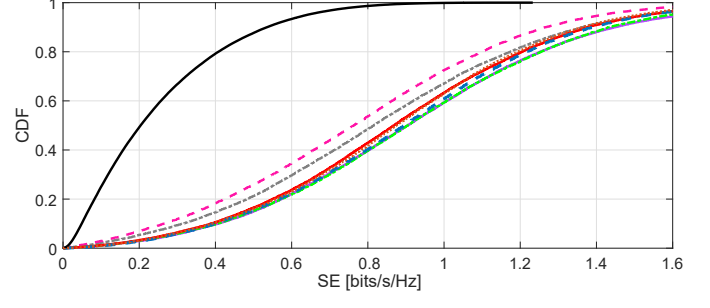
Let us next study the performance of the prior benchmark AP selection algorithms from Sec. IV-C, with the SE shown in

³We have analysed the performance of *UnifSrv-DRL* via extensive simulations under different weights of the reward function i.e., different $\omega_1, \omega_2, \omega_3$, and found that this combination $\omega_1 = 1$, $\omega_2 = 10$, and $\omega_3 = 2000$ achieves the best performance among all considered configurations; we omit the full results for the sake of brevity.

⁴Network planning for optimized AP placement may address this gap, but this is out of our scope.



(a) Seoul network (realistic raytracing channel model)



(b) PPP network (ideal log-distance channel model)

Fig. 5. Spectral efficiency distribution over all UEs and their entire mobility periods with different AP selection algorithms for Seoul and PPP networks, with $M = 324$ APs ($\lambda = 576$ AP/km²).

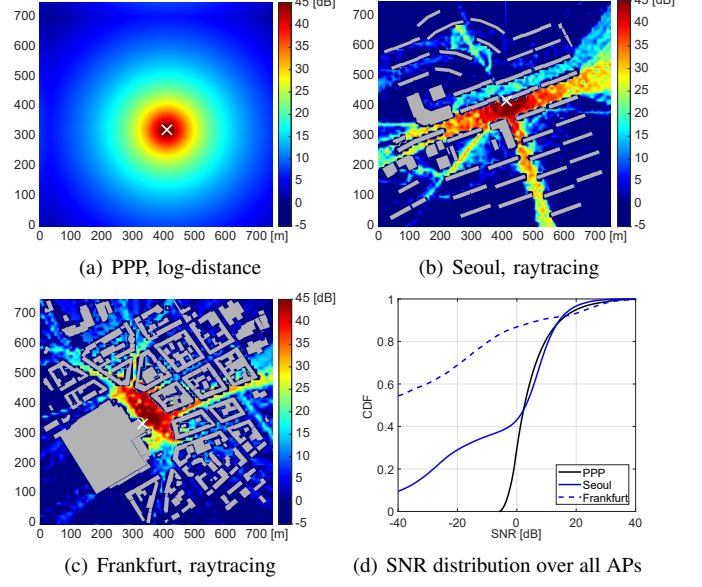
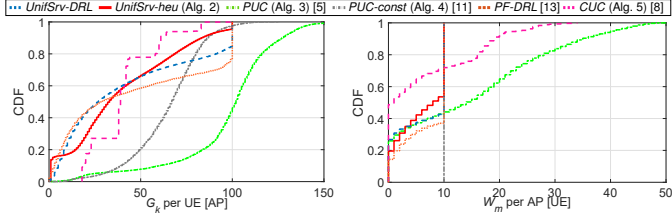


Fig. 6. SNR spatial distribution for different areas and channel models, heatmap for an example AP (white cross) and CDF for all AP-UE channels.

Fig. 5 and the corresponding serving AP set sizes and numbers of served UEs per AP in Fig. 7. To illustrate the serving AP set selection mechanism of all considered algorithms in detail, we show in Fig. 8 the scatter plot of serving AP set size per UE and its corresponding throughput. We furthermore show in Fig. 9 the serving AP set for an example 95th percentile (i.e., worst-served) UE and in Fig. 10 the serving set for an example 10th percentile (i.e., best-served) UE. Fig. 5(b) shows that in the PPP network, all benchmarks achieve a uniformly high throughput close to the original CF-mMIMO upper bound and a significant improvement compared to small cells, validating



(a) serving AP set size per UE, Seoul
 (b) served UEs per AP, Seoul
 (c) serving AP set size per UE, PPP
 (d) served UEs per AP, PPP

Fig. 7. The distribution of serving AP set size per UE and the number of served UEs per AP corresponding to the Seoul and PPP networks in Fig. 5.

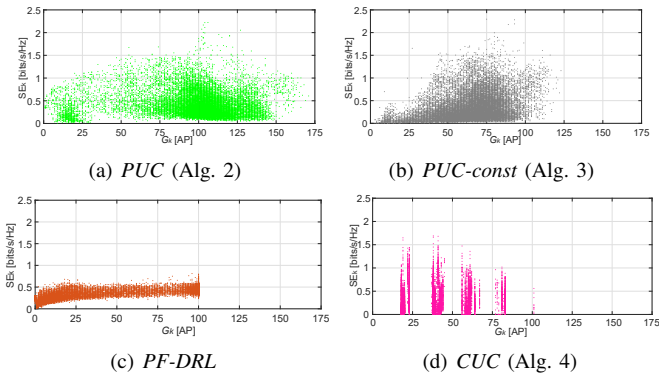


Fig. 8. Scatter plot of serving AP set size versus spectral efficiency with different AP selection algorithms corresponding to the Seoul network in Fig. 5(a).

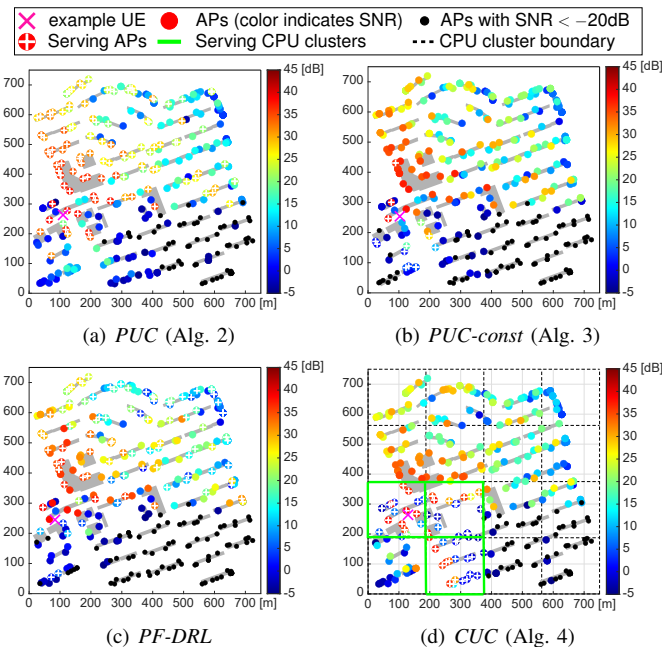


Fig. 9. SNR of example 95%-ile (worst-served) UEs with different AP selection algorithms corresponding to the Seoul network in Fig. 5(a).

the performance of these AP selection schemes in the ideal PPP networks.

Importantly, in the urban network by contrast, Fig. 5(a)

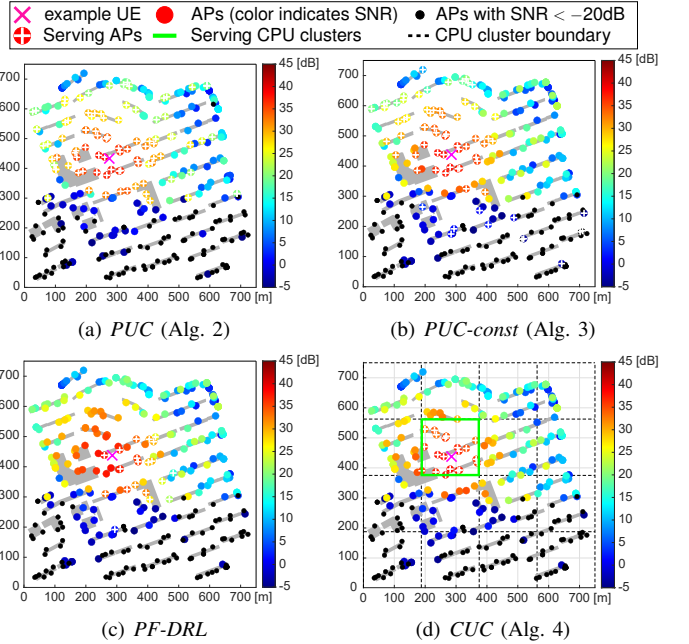


Fig. 10. SNR of to example 10%-ile (best-served) UEs with different AP selection algorithms corresponding to the Seoul network in Fig. 5(a).

shows that among all considered prior benchmarks, only *PUC* achieves a throughput close to the original CF-mMIMO upper bound and similarly high throughput for different serving set sizes (*cf.* Fig. 8(a)). However, Figs. 9(a) and 10(a) show that this is at the cost of a very large serving set size for both worst-served and best-served UEs, violating both the constraints of serving set size G_k and AP capacity W_m , as shown in Figs. 7(a) and 7(b). By contrast, Figs. 7(c) and 7(d) show *PUC* obtains significantly lower serving set size and number of served UEs per AP in the corresponding PPP network than in the urban network in Figs. 7(a) and 7(b). This is because, as Fig. 6(d) shows, the poor channel quality to a large number of candidate serving APs results in a large serving set to achieve a sufficiently good overall serving set quality. The *PUC* algorithm thus fails to select a scalable AP serving set in the realistic urban network.

The *PUC-const* algorithm limits the number of UEs served by an AP and reduces the serving AP set size compared to *PUC*. However, this algorithm prioritizes serving the well-performing UEs by disconnecting the poorly-performing UEs. Consequently, Fig. 8(b) shows that with *PUC-const*, only the UEs with a large serving set size can achieve high throughput. The worst-served UE shown in Fig. 9(b) is only assigned a very small serving set size and APs with bad channel conditions, while the best-served UE in Fig. 10(b) is assigned a very large serving set size. As a result, in the urban network in Fig. 5(a), *PUC-const* slightly improves the performance of the 10% best-served UEs compared to *PUC*, but trades off half of the throughput of the worst-served UEs to satisfy the constraint of AP capacity W_m , leading to a non-uniform throughput performance in the realistic urban network.

Fig. 5(a) shows that the *PF-DRL* algorithm achieves a close throughput performance to *PUC* for the 50% worst-served UEs, but much worse throughput for the 50% best-served UEs. This is because *PF-DRL* only optimizes the proportional fairness of the throughput, where improving the data rate

for the worst-served UEs is prioritized over achieving high peak data rate. This algorithm thus leads to the opposite behavior to *PUC-const*, i.e., improving the throughput of the 50% worst-served UEs, while trading off a large reduction in throughput for the 50% best-served UEs. Correspondingly, Fig. 9(c) shows that *PF-DRL* assigns a very large serving set size to the worst-served UE to achieve good channel conditions of the serving set. Meanwhile, Fig. 10(c) shows that it assigns a very small serving set size to the best-served UEs to satisfy the constraints of serving set size G_k and AP capacity W_m (cf. Figs. 7(a) and 7(b)). Consequently, *PF-DRL* thus obtains low throughput for all serving set sizes (cf. Fig. 8(c)), leading to the large throughput degradation of the top 50% of the UEs compared to the original CF-mMIMO bound shown in Fig. 5(a).

Finally, Fig. 5(a) shows that *CUC* consistently yields poor throughput in the urban network. Fig. 8(d) further shows that with *CUC*, the UEs with a large serving set achieve low throughput compared to others. Fig. 9(d) confirms that the example worst-served UE is assigned to be served by three clusters. However, due to the highly non-uniform channel conditions of urban propagation (cf. Fig. 6(b)), the APs in the same cluster obtain very different channel conditions. These three serving clusters thus do not provide overall good channel quality for the served UE. Moreover, *CUC* also obtain low throughput for the best-served UEs compared to the other three benchmarks. This is because as Fig. 10(d) shows, the example best-served UE is served by only one cluster with good channel conditions due to the constraint of cluster division. *CUC* then cannot select the APs that have good channels but are outside the square serving cluster to further improve the throughput performance as the other three benchmarks.

In summary, although the prior benchmarks perform well in the PPP network, in the realistic Seoul urban network, they either exhibit poor throughput performance (*PUC-const*, *PF-DRL*, and *CUC*) due to failing to assign appropriate APs to the UEs in need, or achieve a good throughput but at the cost of large serving set size due to assigning too many APs (*PUC*). This emphasizes the need for a new AP selection algorithm that jointly optimizes the sum throughput, uniformity of throughput, and serving set size, in order to reach the uniformly good performance of original CF-mMIMO in realistic urban networks, while staying scalable.

B. Performance of the Proposed *UnifSrv* Algorithms

Let us now evaluate the performance of our proposed *UnifSrv* AP selection algorithms. Fig. 5 shows that our *UnifSrv-DRL* algorithm achieves very close throughput performance to the original CF-mMIMO upper bound for all UEs, in both urban and PPP networks. In contrast to *PUC*, which is the only considered benchmark that achieves overall high throughput in the urban network, Figs. 7(a) and 7(c) show that our *UnifSrv* algorithms obtain a similarly small serving AP set size both in the urban and PPP networks. Compared to the prior benchmarks *PUC-const* and *CUC* that partially satisfy the constraints of serving set size G_k and AP capacity W_m , *UnifSrv-DRL* achieves significantly higher throughput for the 95th percentile (i.e., worst-served) UEs. Furthermore, compared to the benchmark *PF-DRL*, which is the only considered scheme other than our *UnifSrv* algorithms

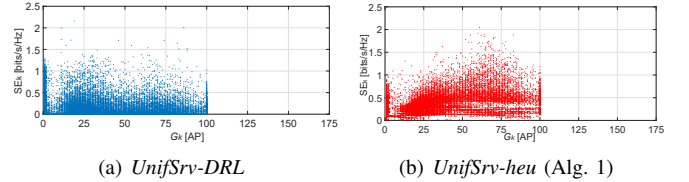


Fig. 11. Scatter plot of serving AP set size versus spectral efficiency with *UnifSrv* corresponding to the networks in Fig. 5(a).

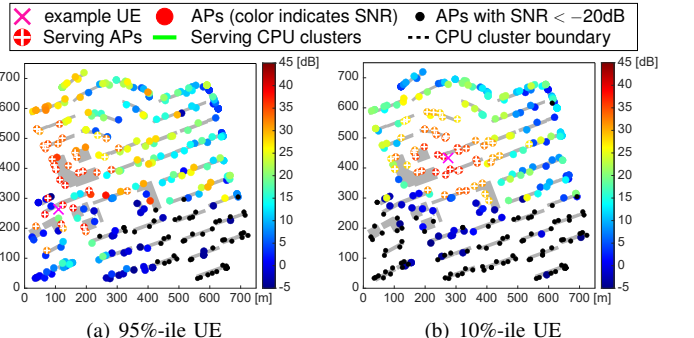


Fig. 12. SNR of an example 95%-ile UE and 10%-ile UE with *UnifSrv* corresponding to the networks in Fig. 5(a).

that satisfies both the constraints of $G_k \leq G_{max}$ (Fig. 7(a)) and $W_m \leq \tau_p$ (Fig. 7(b)), *UnifSrv-DRL* achieves significantly higher throughput for the 50% best-served UEs, and therefore achieves higher sum throughput over the network. Fig. 5(a) also shows that our *UnifSrv-heu* heuristic algorithm achieves a comparable throughput performance to *UnifSrv-DRL*, due to exhibiting a similar AP selection behavior, as illustrated in Figs. 7(a) and 7(b). Therefore, unlike all prior benchmarks, both our *UnifSrv* algorithms successfully achieve *uniformly good* throughput performance close to the original CF-mMIMO upper bound in the urban network, with a minimized serving set size, ensuring scalability.

We underline that the superior performance of our *UnifSrv* algorithms comes from the focus on jointly improving both the throughput performance itself and the throughput fairness over the network, by making both the sum data rate (10a) and fairness index (10b) objectives in our optimization problem in (10). As a result, our *UnifSrv* algorithms significantly improve the performance of the worst-served UEs, while only trading off a very small amount of data rate (throughput difference with *PUC* being less than 0.1 bits/s/Hz) of the best-served UEs to satisfy the G_{max} constraint and obtain a small serving set size of on average 25 APs. Fig. 7(a) further shows that compared to the PPP network in Fig. 7(c), our *UnifSrv* algorithms in the urban network result in a wider distribution of serving set size per UE with the same average G value. This illustrates that our algorithms achieve their good throughput performance in the non-uniform urban environment by appropriately distributing serving APs over the UEs based on channel conditions and system cost constraints.

We further illustrate the AP selection of *UnifSrv* with the scatter plot in Fig. 11 and the example serving APs⁵ in Fig. 12. Both our *UnifSrv-DRL* algorithm in Fig. 11(a) and our *UnifSrv-heu* algorithm in Fig. 11(b) achieve similar

⁵We note that our *UnifSrv-heu* algorithm forms very similar serving AP sets as *UnifSrv-DRL* for the example UEs in Fig. 12. We thus show the results for *UnifSrv-DRL* as a representative for both our *UnifSrv* algorithms in Fig. 12.

throughput for different serving set sizes. Fig. 12 shows that our *UnifSrv* algorithms do so by successfully assigning the serving APs with near-optimal channel conditions to serve different UEs. For both the worst-served UE in Fig. 12(a) and best-served UE in Fig. 12(b), the serving set is always composed of a small number of APs with good channel conditions. Our *UnifSrv-DRL* algorithm selects the optimal serving set by maximizing the reward function given in (13), which maximizes both the total data rate and fairness index, while our *UnifSrv-heu* algorithm does so by introducing a fairness index-based threshold to control the serving AP set expansion. In contrast to the prior benchmarks discussed in Sec. V-A that only partially consider the objectives and constraints in (10), our *UnifSrv* algorithms jointly maximize both the throughput and the fairness of the throughput per UE, minimize the serving set size, and satisfy both the constraints of serving set size and AP capacity. Therefore, as shown in Figs. 11 and 12, our *UnifSrv* algorithms assign the serving APs with both the appropriate quantity and quality to each UE, thus achieving *uniformly good* throughput in realistic urban networks shown in Fig. 5(a).

Finally, we study the performance of CF-mMIMO in Frankfurt (c.f. Figs. 1(b) and 6(c)), which represents an even more non-uniform urban propagation environment than Seoul, with narrower streets and more pronounced shadowing and urban canyon effects. Fig. 13 shows that the throughput performance trends in Frankfurt are similar to those for Seoul in Fig. 5(a) and that our *UnifSrv* algorithms also achieve throughput close to the original CF-mMIMO upper bound. Fig. 13 shows that in Frankfurt, the *CUC* algorithm performs worse than in Seoul, resulting in CF-mMIMO performing *worse* than small cells for around 40% of UEs. Furthermore, with the *PF-DRL* algorithm, more UEs (around 80%) obtain worse throughput than *UnifSrv* and *PUC*, although Fig. 14 shows that *PF-DRL* selects similarly large serving set sizes as *UnifSrv-DRL*. This indicates that *PF-DRL* tends to assign more APs to serve the worst-served UEs in order to compensate the overall poorer channel conditions in Frankfurt (c.f. Fig. 6(d)), while leaving more UEs with insufficient serving sets. This emphasizes that it is not sufficient to solely optimize the proportional fairness of the throughput as *PF-DRL* does. Importantly, Figs. 13 and 14 show that both our *UnifSrv-DRL* and *UnifSrv-heu* achieve comparable throughput while satisfying the constraints of G_{max} and W_{max} also in Frankfurt. Fig. 14(a) shows that the DRL solution *UnifSrv-DRL* tends to choose a slightly larger serving set size compared to the heuristic *UnifSrv-heu*. This is because in Frankfurt, the channel quality is in general very poor (c.f. Fig. 6(d)), so that the agent requires more serving APs per UE to achieve a high total reward of r_1 . We note that due to this slightly larger serving set size, *UnifSrv-DRL* achieves slightly better throughput for the 15%-likely UEs than *UnifSrv-heu* in Frankfurt.

C. Comparative Evaluation of Performance & Complexity

In this section, we summarize our evaluation of all considered AP selection algorithms from the angle of the optimization problem formulation in Sec. IV-A and algorithm complexity to determine the recommended AP selection algorithm for CF-mMIMO for practical urban mobile networks.

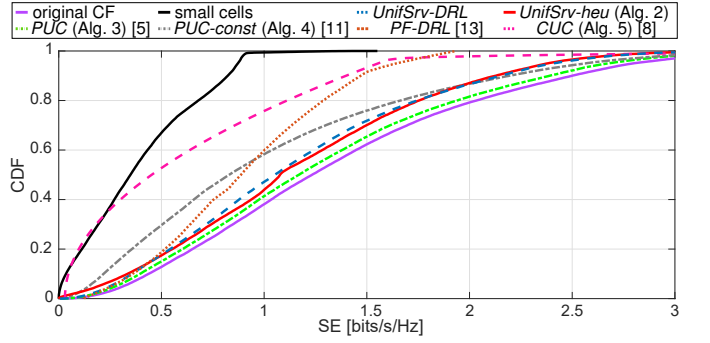


Fig. 13. Spectral efficiency distribution over all UEs and their entire mobility periods with different AP selection algorithms for the Frankfurt network, with $M = 625$ APs ($\lambda = 1111$ AP/km 2).

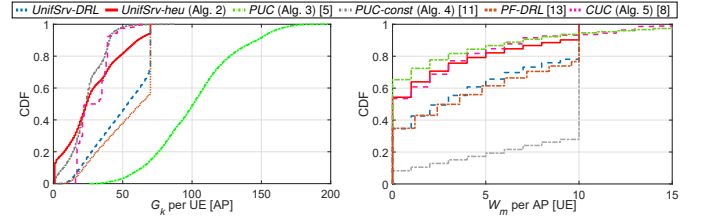
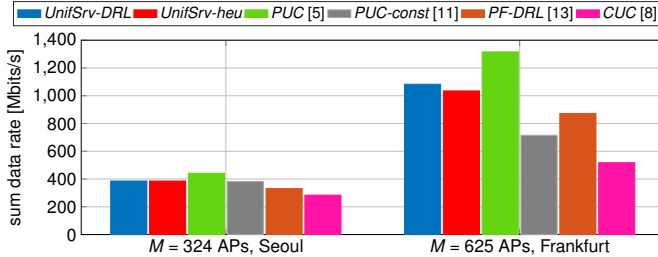
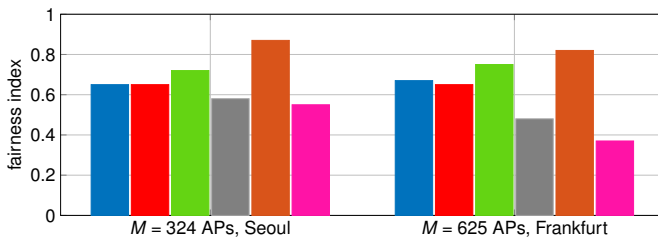
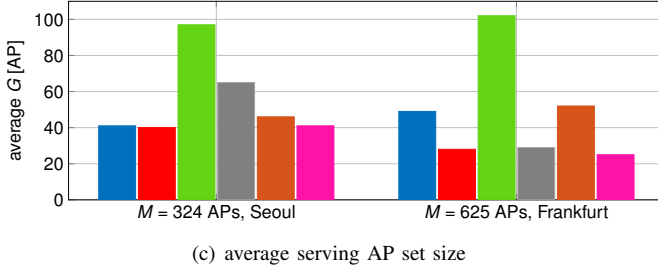


Fig. 14. The distribution of serving AP set size per UE and the number of served UEs per AP corresponding to the Frankfurt networks in Fig. 13.

We show in Fig. 15 the objective values and in Table IV the constraints given by (10) for all considered AP selection algorithms in Seoul and Frankfurt. All four benchmarks satisfy only a part of the objectives or constraints in our optimization problem (10). Fig. 15(a) shows that the *PUC* algorithm achieves the highest data rate in both cities, but at the cost of also the largest serving set size (c.f. Fig. 15(c)) and the violation of both constraints (c.f. Table IV). The *PUC-const* algorithm satisfies the AP capacity limit, but Fig. 15(a) shows that it achieves similar and lower throughput compared to our *UnifSrv* in Seoul and Frankfurt, respectively. Furthermore, Fig. 15(b) shows that its fairness index value is low, indicating the per-UE throughput performance is not uniform. Importantly, Figs. 5(a) and 13 show that this low fairness index comes from the high throughput for the best-served UEs and low throughput for the worst-served ones, which is the opposite of the original design goal of CF-mMIMO. Fig. 15(b) shows that the *PF-DRL* algorithm achieves the highest fairness index and satisfies both constraints (c.f. Table IV), indicating a uniform throughput performance over the network. However, Fig. 15(a) shows that its data rate is significantly lower than our *UnifSrv* and *PUC* in both cities (c.f. Fig. 15(a)). The *PF-DRL* algorithm thus does not fulfill the goal of CF-mMIMO to achieve both *high* and *uniform* throughput. Instead, Figs. 5(a) and 13 show that *PF-DRL* trades off the throughput of the top 60% of UEs for a high fairness index. Fig. 15(c) shows that the *CUC* algorithm obtains the lowest serving set size in both cities and satisfies the constraint of G_{max} . However, both its throughput (c.f. Fig. 15(a)) and fairness index value (c.f. Fig. 15(b)) are low in both cities, and therefore the throughput is neither high nor uniform. Importantly, Fig. 15 and Table IV show that only our *UnifSrv* algorithms successfully achieve high throughput, high fairness index, and low serving set



(a) sum data rate

(b) fairness index Φ 

(c) average serving AP set size

Fig. 15. The objective values of all algorithms in Seoul and Frankfurt.

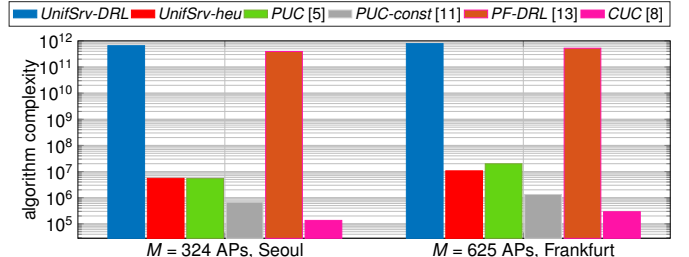


Fig. 16. The algorithm complexity of all algorithms in Seoul and Frankfurt.

at the cost of poor throughput performance (cf. Fig. 15(a)). We note that prior works with DRL solutions, e.g., [13, 18] consider the much lower complexity of prediction of a trained agent instead of training complexity, because the agent only needs to be trained once for a network and then can be run offline. However, the state and action space of a DRL solution is designed for a specific network deployment. Therefore, a trained agent for an urban network is highly unlikely to perform well in other networks and is required to be re-trained, since the network topology and propagation in different urban areas are likely to be highly different. By contrast, our *UniSrv-heu* algorithm can be directly applied in any topology and propagation, like the other heuristic benchmarks (*PUC*, *PUC-const*, and *CUC*). Fig. 16 shows that the *CUC* algorithm entails the lowest complexity, but Figs. 5(a), 13, and 15 show that it also obtains the worst throughput and fairness performance. By contrast, our *UniSrv-heu* algorithm entails comparable complexity to *CUC*, but with significantly better throughput, as shown in Figs. 5(a) and 13. Importantly, *UniSrv-heu* achieves almost equivalent throughput performance to *UniSrv-DRL* but with orders of magnitude lower complexity, and is thus recommended for practical urban CF-mMIMO network deployments.

TABLE IV
CONSTRAINTS OF DIFFERENT AP SELECTION ALGORITHMS

Algorithms	Serving Set Constraint G_{\max} Met?	AP Capacity Constraint W_{\max} Met?
<i>PUC</i> (Alg. 2 [5])	No	No
<i>PUC-const</i> (Alg. 3 [11])	No	Yes
<i>PF-DRL</i> [13]	Yes	Yes
<i>CUC</i> (Alg. 4 [8])	Yes	No
<i>UniSrv-DRL</i>	Yes	Yes
<i>UniSrv-heu</i>	Yes	Yes

size, with both constraints satisfied in both urban networks.

Lastly, we compare the complexity of these algorithms by presenting in Fig. 16 the quantified algorithm complexity in Table III for both considered numbers of APs. The training for both *UniSrv-DRL* and *PF-DRL* was done on a server with GPU NVIDIA Quadro RTX 5000. The number of episodes to converge N is recorded as: $N = 250$ for *UniSrv-DRL* in Seoul; $N = 300$ for *UniSrv-DRL* in Frankfurt; $N = 150$ for *PF-DRL* in Seoul; $N = 200$ for *PF-DRL* in Frankfurt. All algorithms obtain higher complexity in the area of Frankfurt than in Seoul, due to the higher AP density in Frankfurt. For both cities, Fig. 16 shows that the two DRL-based algorithms *UniSrv-DRL* and *PF-DRL* entail orders of magnitude higher complexity compared to other algorithms, due to the high dimension of neural network layers and the large number of steps to converge. *PF-DRL* obtains slightly lower complexity than *UniSrv-DRL*, because the single optimization objective of proportional fairness leads to a smaller number of episodes to converge. However, this slight decrease in complexity is

VI. CONCLUSIONS

We conducted a comprehensive performance analysis of CF-mMIMO under realistic urban propagation and proposed the AP selection algorithms *UniSrv* to achieve uniformly good performance for CF-mMIMO under the highly non-uniform realistic urban environment. We quantified the uniformity of throughput performance via Jain's fairness index and formulated a multi-objective optimization problem to jointly maximize both the sum data rate and the fairness index of the data rate per UE, while minimizing the number of AP - UE connections and thus minimizing the system cost. To solve the optimization problem, we proposed both a DRL and a heuristic AP selection algorithm. We presented extensive simulations to show our *UniSrv* algorithms significantly outperform all considered benchmarks, and thus for the first time achieve both high and uniform throughput of CF-mMIMO in realistic urban environments. Importantly, our heuristic algorithm *UniSrv-heu* achieves very similar performance to the DRL solution *UniSrv-DRL*, but with orders of magnitude lower complexity, making it an attractive solution for practical CF-mMIMO. Our ongoing work is on jointly optimizing the throughput and mobility management cost, i.e., handover overheads, of mobile CF-mMIMO in practical deployments.

Algorithm 2 pure UE-centric (PUC) [5]

Input: The SNR β_{mk} between AP m and UE k for $m = 1, \dots, M$ and $k = 1, \dots, K$. The zero matrix $D[t] = \mathbf{0}$. The SNR percentage threshold δ .

```

1: for  $k = 1, \dots, K$  do
2:   Perform Steps 2 to 3 in Alg. 1.
3:   for  $m = 1, \dots, M$  do
4:     if  $\sum_{m=1}^M D_{mk} \beta_{mk} < \delta \sum_{m=1}^M \beta_{mk}$  then
5:       Set  $D_{O(m)k} = 1$ .
6:     else
7:       break
8:     end if
9:   end for
10: end for

```

Output: The dynamic cooperation matrix D .

Algorithm 3 constrained pure UE-centric (PUC-const.) [11]

Input: The SNR β_{mk} between AP m and UE k for $m = 1, \dots, M$ and $k = 1, \dots, K$. The zero matrix $D[t] = \mathbf{0}$. The pilot sequence length τ_p .

```

1: for  $k = 1, \dots, K$  do
2:   Perform Steps 2 to 3 in Alg. 1.
3:   for  $m = 1, \dots, M$  do
4:     if  $W_m \leq \tau_p$  then
5:       Set  $D_{O(m)k} = 1$ .
6:     else
7:       Find the UE with the worst channel among all
       current candidate UEs of AP  $m$ ,  $k^* = \arg \min_{i \in W_m} \beta_{im}$ .
8:       if  $\beta_{k^*m} < \beta_{km}$  then
9:         Set  $D_{k^*m} = 0$ ,  $D_{km} = 1$ .
10:      end if
11:    end if
12:   end for
13: end for

```

Output: The dynamic cooperation matrix D .

APPENDIX

PSEUDOCODE FOR REFERENCE ALGORITHMS

We here give the detailed pseudocode for the *PUC*, *PUC-const*, and *CUC* reference AP selection algorithms.

REFERENCES

- [1] H. Q. Ngo *et al.*, “Cell-free massive MIMO versus small cells,” *IEEE Trans. Wireless Commun.*, vol. 16, no. 3, pp. 1834–1850, 2017.
- [2] H. Claussen *et al.*, *Small cell networks: deployment, management, and optimization*. John Wiley & Sons, 2017.
- [3] T. Demir, E. Björnson, and L. Sanguinetti, *Foundations of user-centric cell-free massive MIMO*, 2021.
- [4] S. Buzzi and C. D’Andrea, “Cell-free massive MIMO: user-centric approach,” *IEEE Wireless Commun. Lett.*, vol. 6, 2017.
- [5] H. Q. Ngo *et al.*, “On the total energy efficiency of cell-free massive MIMO,” *IEEE Trans. Green Commun. Netw.*, vol. 2, 2018.
- [6] Z. Gao *et al.*, “DRL-based AP selection in downlink cell-free massive MIMO network with pilot contamination,” *IEEE Commun. Lett.*, vol. 28, 2024.
- [7] B. Banerjee *et al.*, “Access point clustering in cell-free massive MIMO using conventional and federated multi-agent reinforcement learning,” *IEEE Trans. Mach. Learn. Commun. Netw.*, vol. 1, 2023.
- [8] G. Interdonato, P. Frenger, and E. G. Larsson, “Scalability aspects of cell-free massive MIMO,” in *Proc. IEEE ICC*, Shanghai, 2019.
- [9] P. Biswas *et al.*, “Optimal access point centric clustering for cell-free massive MIMO using Gaussian mixture model clustering,” *IEEE Trans. Mach. Learn. Commun. Netw.*, vol. 2, 2024.
- [10] C. F. Mendoza *et al.*, “User-centric clustering in cell-free MIMO networks using deep reinforcement learning,” in *Proc. IEEE ICC*, Rome, 2023.
- [11] S. Chen *et al.*, “Wireless powered IoE for 6G: Massive access meets scalable cell-free massive MIMO,” *China Commun.*, vol. 17, no. 12, pp. 92–109, 2020.
- [12] Y. Xiao and L. Simić, “Performance of cell-free massive MIMO in realistic urban propagation environments,” in *Proc. IEEE WCNC*, Milan, 2025.
- [13] A. Prado *et al.*, “Enabling proportionally-fair mobility management with reinforcement learning in 5G networks,” *IEEE J. Sel. Areas Commun.*, vol. 41, 2023.
- [14] Y. Xiao, P. Mähönen, and L. Simić, “Poster abstract: Performance of scalable cell-free massive MIMO in practical network topologies,” in *Proc. IEEE INFOCOM*, Hoboken, NJ, USA, 2023.
- [15] M. Zaher *et al.*, “Soft handover procedures in mmWave cell-free massive MIMO networks,” *IEEE Trans. Wireless Commun.*, vol. 23, no. 6, pp. 6124–6138, 2024.
- [16] D. Löschkenbrand *et al.*, “Towards cell-free massive MIMO: a measurement-based analysis,” *IEEE Access*, vol. 10, 2022.
- [17] P. H. T. D. Silva, R. Duarte, H. S. Silva, M. Alencar, and W. J. L. D. Queiroz, “Evaluation of cell-free millimeter-wave massive MIMO systems based on site-specific ray tracing simulations,” *IEEE Access*, vol. 10, 2022.
- [18] Y. Tsukamoto *et al.*, “Scalable AP clustering with deep reinforcement learning for cell-free massive MIMO,” *IEEE Open J. Commun. Soc.*, vol. 6, 2025.
- [19] Y. Cao *et al.*, “Implementation of a cell-free RAN system with distributed cooperative transceivers under ORAN architecture,” *IEEE J. Sel. Areas Commun.*, vol. 43, 2025.
- [20] (2024) OpenStreetMap data extracts. [Online]. Available: <https://download.geofabrik.de/>
- [21] H. A. Ammar *et al.*, “Handoffs in user-centric cell-free MIMO networks: a POMDP framework,” *IEEE Trans. Wireless Commun.*, vol. 23, 2024.
- [22] R. Beerten *et al.*, “Mobile cell-free massive MIMO: a practical O-RAN-based approach,” *IEEE Open J. Commun. Soc.*, vol. 6, pp. 593–610, 2025.
- [23] I. Kim, R. Galiza, and L. Ferreira, “Modeling pedestrian queuing using micro-simulation,” *Transportation Research Part A: Policy and Practice*, vol. 49, pp. 232–240, 2013.
- [24] X. Lin *et al.*, “Towards understanding the fundamentals of mobility in cellular networks,” *IEEE Trans. Wireless Commun.*, vol. 12, no. 4, pp. 1686–1698, 2013.
- [25] E. Björnson and L. Sanguinetti, “Scalable cell-free massive MIMO systems,” *IEEE Trans. Commun.*, vol. 68, no. 7, pp. 4247–4261, 2020.
- [26] J. Zheng *et al.*, “Impact of channel aging on cell-free massive MIMO over spatially correlated channels,” *IEEE Trans. Wireless Commun.*, vol. 20, no. 10, pp. 6451–6466, 2021.
- [27] P. Mededovic, M. Vletic, and Z. Blagojevic, “Wireless insite software verification via analysis and comparison of simulation and measurement results,” in *Proc. MIPRO*, Opatija, 2012.
- [28] A. B. Sediq *et al.*, “Optimal tradeoff between sum-rate efficiency and Jain’s fairness index in resource allocation,” *IEEE Trans. Wireless Commun.*, vol. 12, 2013.